International Journal of Biochemistry and Cell Biology 112 (2019) 39–49

Contents lists available at ScienceDirect

International Journal of Biochemistry and Cell Biology

journal homepage: www.elsevier.com/locate/biocel

A positive feedback loop of miR-30a-5p-WWP1-NF-κB in the regulation of glioma development

Peichao Zhao*, MengMeng Wang, Jiyang An, Hongwei Sun, Tianhao Li, Dongming Li

Department of Neurosurgery, The First Affiliated Hospital of Zhengzhou University, Zhengzhou, 450000, Henan Province, China

ARTICLE INFO

Keywords:
WWP1
miR-30a-5p
NF-κB p65
Glioma

ABSTRACT

Previous studies demonstrated that miR-30a-5p promotes glioma cell growth and invasion. Furthermore, WWP1 (WW domain containing E3 ubiquitin protein ligase 1) inhibits NF-κB activation that is strongly correlated with gliomagenesis. Using the GEO database and bioinformatics analyses, we identified WWP1 was downregulated in glioma tissues and might be a putative target for miR-30a-5p. Hence, this study aims to explore the interaction among miR-30a-5p, WWP1, and NF-κB and their roles in the regulation of glioma development. We found decreased WWP and increased miR-30a-5p expression and p65 phosphorylation in glioma tissues. Furthermore, WWP1 mRNA level was negatively correlated with miR-30a-5p expression in glioma tissues. Interestingly, miR-30a-5p targeted WWP1 expression. Additionally, NF-κB p65 overexpression increased miR-30a-5p expression through direct binding of NF-κB RelA subunit to the promoter of miR-30a-5p. We also confirmed that WWP1 overexpression decreased phosphorylation of NF-κB p65. Importantly, miR-30a-5p promoted glioma cell proliferation, migration, and invasion via targeting WWP1. Furthermore, NF-κB p65 overexpression inhibited WWP1 expression and promoted glioma cell malignant behaviors via inducing miR-30a-5p transcription. Moreover, WWP1 overexpression decreased miR-30a-5p expression and inhibited glioma cell malignant behaviors via inhibiting NF-κB p65. Our further assay showed that WWP1 inhibited *in vivo* growth of xenograft tumors of glioma cells, accompanied with a decrease in miR-30-5p expression and phosphorylation of NF-κB p65. In conclusion, there is a "miR-30a-5p-WWP1-NF-κB" positive feedback loop, which plays an important role in regulating glioma development and might provide a potential therapeutic strategy for treating glioma.

1. Introduction

Glioma is the most common and aggressive primary brain tumor in adults with high morbidity and mortality (DeWitt et al., 2017). Despite significant progress in the treatment, the prognosis of patients with glioma is still unfavorable (Huang et al., 2017). Thus, it is imperative to clarify the molecular mechanism underlying glioma development and develop more appropriate therapeutic targets for the treatment of glioma.

The gene for E3 ubiquitin ligase WWP1 (WW domain containing E3 ubiquitin protein ligase 1) is located at 8q21, a region frequently amplified in human cancers (Chen et al., 2007). WWP1 has been shown to be dysregulated in diverse cancers such as prostate cancer (Goto et al., 2016), gastric cancer (Ma et al., 2018a), and colorectal cancer (Chen and Zhang, 2018). Interestingly, we observed that WWP1 expression was significantly downregulated in glioma tissues compared with the normal brain tissues using the GEO database analysis (GDS4467/GSE15824). However, the role of WWP1 in glioma development remains unclear.

NF-κB mediates inflammatory response involved in various biological processes such as immune regulation and tumorigenesis (Allen et al., 2012; Ma et al., 2018b; van Delft et al., 2015). Increasing evidence has indicated a strong correlation between constitutive NF-κB activation and gliomagenesis (Atkinson et al., 2010). Of note, previous studies have revealed that WWP1 inhibits LPS-induced NF-κB activation by inducing K48-linked polyubiquitination of endogenous TNF receptor-associated factor 6 (TRAF6) (Lin et al., 2013). Therefore, it is possible that WWP1 may play a role in regulating glioma development by inhibiting NF-κB.

MicroRNAs (miRNAs) are negative regulators of gene expression by binding to the 3′-untranslated region (3′-UTR) of target mRNAs (Deyao et al., 2014). Our bioinformatics analysis revealed that WWP1 was a putative target of miR-30a-5p by harboring miR-30a-5p binding sequences in the 3′-UTR of its mRNA (Targetscan). Previous studies have

* Corresponding author at: Department of Neurosurgery, The First Affiliated Hospital of Zhengzhou University, No.1 Jianshedong Road, Zhengzhou, 450000, Henan Province, China.
E-mail address: zhaopc2009@163.com (P. Zhao).

https://doi.org/10.1016/j.biocel.2019.04.003
Received 30 January 2019; Received in revised form 22 March 2019; Accepted 8 April 2019
Available online 10 April 2019
1357-2725/ © 2019 Published by Elsevier Ltd.

demonstrated that miR-30a-5p promotes glioma cell growth and invasion (Jia et al., 2013; Wang et al., 2015). These findings suggest that WWP1 may be involved in the gliomagenesis-promoting role of miR-30a-5p.

NF-κB is a pleiotropic transcription regulator that is activated by various intra- and extra-cellular stimuli (O'Dea and Hoffmann (2010)). Studies have shown that NF-κB can participate in tumor development by regulating the transcription of certain miRNAs (Li et al., 2017; Shuang et al., 2017; Wang et al., 2018). Our bioinformatics analysis revealed that NF-κB RELA subunit is a potential transcriptional factor for miR-30a (DIANA Tools). Thus, we hypothesized that NF-κB activation in glioma might induce transcription of miR-30a-5p and thereby promote glioma development.

Based on the above-mentioned findings, we speculated a possible feedback loop of miR-30a-5p-WWP1-NF-κB in regulating gliomagenesis. To address this, we investigated the interaction among miR-30a-5p, WWP1, and NF-κB. Furthermore, we determined the role of the miR-30a-5p-WWP1-NF-κB axis in regulating glioma development.

2. Materials and methods

2.1. Ethics statement and sample collection

This study was approved by the Research Ethics Committee of The First Affiliated Hospital of Zhengzhou University. Written informed consent was obtained from each participant. Glioma was diagnosed according to 2000 WHO criteria. All pathological sections were analyzed by two independent pathologists. The normal brain tissues were obtained from patients with craniocerebral trauma who underwent resection during surgery in the same hospital and were proven pathologically to be normal brain tissues. Glioma tissues (n = 25) and normal brain tissues (n = 20) were collected immediately after the surgical removal, and snap-frozen in liquid nitrogen for subsequent analysis.

2.2. Cell culture

Four glioma cell lines (U87, U251, U138, LN229) and normal human astrocytes (NHA) were purchased from the American Type Culture Collection (ATCC, Manassas, VA, USA). Cells were cultured in Dulbecco's modified Eagle's medium (DMEM; Thermo Fisher Scientific, Inc., Waltham, MA, USA) supplemented with 10% fetal bovine serum (FBS, Gibco; Thermo Fisher Scientific, Inc.) and antibiotics (100 U/mL penicillin and 100 mg/mL streptomycin). Cells were maintained in humidified air with 5% CO_2 at 37 °C.

2.3. Cell transfection

To overexpress WWP1 or p65, the cDNAs encoding WWP1 or p65 were inserted into pcDNA 3.1 (Invitrogen; Thermo Fisher Scientific, Inc.), generating pcDNA3.1-WWP1 or pcDNA3.1-p65. An empty pcDNA3.1 vector served as a control. The miR-30a-5p mimics, miR-30a-5p inhibitors, and their corresponding controls were purchased from GenePharma (Shanghai, China). When cells confluence reached 80–90%, cells were transfected with these plasmids using Lipofectamine™ 2000 (Invitrogen) according to the manufacturer's instructions.

2.4. Luciferase reporter assay

To determine whether WWP1 3′-UTR was directly targeted by miR-30a-5p, the WWP1 3′-UTR containing the predicted wild-type (WT) binding sites of miR-30a-5p or mutated miR-30a-5p binding sites (MUT) were amplified by PCR and cloned into a pGL3 vector, termed as WWP1-WT, and WWP1-MUT. For luciferase assay, cells were co-transfected with WWP1-WT or WWP1-MUT, and miR-30a-5p mimic or negative control miRNA mimic (mimic NC) by Lipofectamine 2000 (Invitrogen). At 24 h post transfection, the luciferase activities were analyzed using a luciferase reporter assay system (Promega Corporation, Fitchburg, WI, USA).

To determine whether NF-κB could bind to the promoter of miR-30a-5p, the miR-30a-5p promoter region containing the predicted wild-type (WT) NF-κB RelA-binding site or mutated (Mut) NF-κB RelA-binding site was amplified by PCR and cloned into a pGL3 vector. For luciferase assay, cells were co-transfected with the reporter plasmids and pcDNA3.1- NF-κB RelA plasmid. Luciferase activity was measured using a luciferase reporter assay system (Promega Corporation) according to the manufacturer's instructions.

2.5. Chromatin immunoprecipitation (ChIP) assay

ChIP assay was performed to test the binding of NF-κB p65 to the miR-30a-5p promoter as previously described (Ku et al., 2017), with some alterations. Briefly, the cells were trypsinized and resuspended in lysis buffer, and nuclei were isolated and sonicated to obtain DNA lysates. The samples were centrifuged, and the supernatants were diluted with ChIP dilution buffer. The samples were subsequently precleared to reduce the nonspecific background and then incubated with primary antibody (anti-NF-κB p65) overnight. Antibody-bound protein/DNA complexes were eluted. DNA was purified using the QIAquick PCR Purification Kit (Qiagen, USA) and subjected to PCR analysis. IgG was used as a negative control.

2.6. Cell proliferation, migration, and invasion assay

For cell proliferation assay, cells were plated into 96-well plates at a density of 2×10^3 cells in 200 μL/well. Cell proliferation was determined using the MTT Cell Proliferation Kit (Beyotime, Shanghai, China) according to the manufacturer's protocol. Cellular viability was determined by detecting the optical density (OD) at a wavelength of 490 nm using a microplate autoreader (EL309; BioTek Instruments, Inc., Winooski, VT, USA).

Transwell cell culture chambers were used to examine cell migration and invasion assay. Briefly, cells (2×10^4) were suspended in serum-free DMEM medium (200 μL) and was then added to the upper chamber, while full-serum medium containing DMEM with 10% FBS (600 μL) was added to the bottom chamber of the 24-well chamber as a chemoattractant. Cells were allowed to migrate through the membranes for 24 h. After that, cells adhering to the bottom side were washed with PBS, fixed with methanol, and then stained with 0.1% crystal violet for 30 min. Finally, the stained cells were photographed under a microscope (Nikon E100; Nikon Corp, Tokyo, Japan) and cell number was counted from 5 random fields of each well. The same procedures were followed for the invasion assay, except that diluted Matrigel (BD Biosciences, San Jose, CA, USA) were precoated on the upper well of the transwell chamber.

2.7. Establishment of LN229 cells stably transfected with WWP1

When the cell confluence reached 80%, the LN229 cells were transfected with pcDNA3.1-WWP1 or empty pcDNA3.1 vector. Subsequently, 2 μg of plasmid DNA and 6 μL of FuGENE HD transfection reagent (Promega, China) were added to 100 μL of Opti-MEM medium. Following 15 min of incubation at room temperature, 100 μL of plasmid DNA-containing mixture was added to each well for 48 h of incubation. After screening for 4 weeks in a selective medium containing G418 (400 mg/L), the G418-resistant colonies were obtained, and the LN229 cells stably transfected with WWP1 were obtained following culture expansion.

2.8. Xenografted tumors in nude mice

BALB/c nude mice (weight, 16–20 g; age, 5–6 weeks old) were

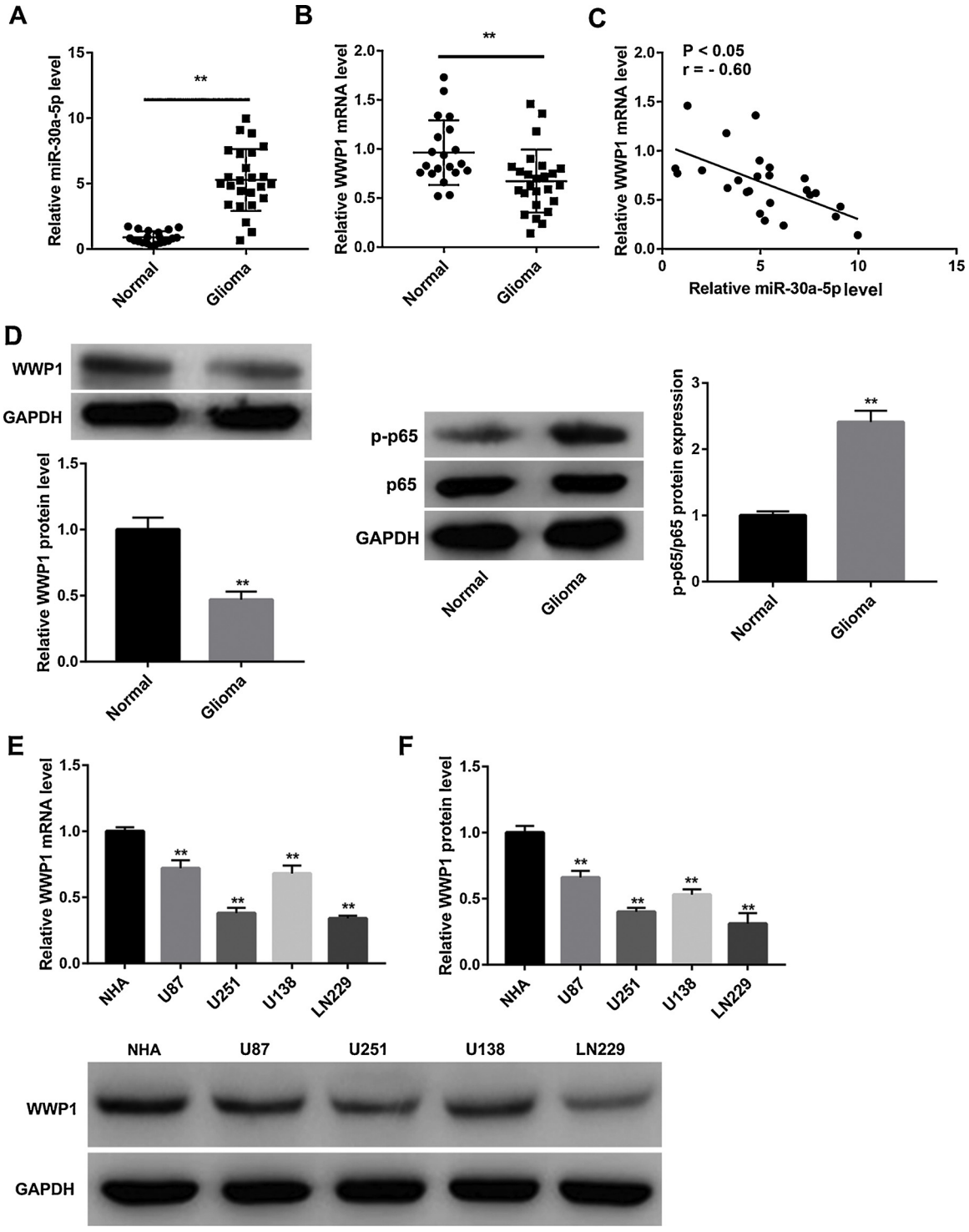

Fig. 1. Expression of WWP1, miR-30a-5p, and p-p65 in glioma tissues.
Relative miR-30a-5p expression (A) and WWP1 mRNA levels (B) in normal brain tissues (n = 20) and human glioma tissues (n = 25) were measured by qRT-PCR. (C) WWP1 mRNA level was negatively correlated with miR-30a-5p expression in glioma tissues (Pearman test). (D) The protein levels of WWP1, p65, phosphorylated (p)-p65 in human glioma tissues and normal brain tissues were measured by western blot. The mRNA (E) and protein (F) levels of WWP1 in four glioma cell lines (U87, U251, U138, LN229) and normal human astrocytes (NHA) were measured by qRT-PCR and western blot respectively. $^{**}P < 0.01$ vs. Normal or NHA group. Results are expressed as mean ± SD for three independent experiments.

raised under the specific pathogen-free environment (temperature, 25 ± 2 °C; humidity, 45–50%), with free access to food and water. All animal experiments were performed in strict accordance with the guidelines for the Care and Use of Laboratory Animals of the National Institutes of Health. This study was approved by the Ethics Committee of The First Affiliated Hospital of Zhengzhou University.

The mice were randomly divided into two groups (n = 4 for each group): Empty vector and WWP1 OE. The LN229 cells stably transfected with pcDNA3.1-WWP1 (WWP1 OE group) or empty pcDNA3.1 vector (Empty vector group) were digested with 0.25% trypsin, followed by centrifugation. Following removal for supernatant, the resulting pellets were suspended in serum-free DMEM medium and the final

concentration was adjusted to 1×10^6 cells in 50 μL serum-free DMEM medium. After that, cell suspension was injected subcutaneously into the position between left leg and abdominal cavity of each mouse. The longest dimension (a, mm) and perpendicular width (b, mm) were measured with a caliper, and tumor volume (V, mm^3) was calculated following the formula: $V = (ab^2)/2$. Thirty-five days later, mice were sacrificed under anesthesia and the tumors were separated.

2.9. Hematoxylin and eosin (H&E) staining

H&E staining was performed to evaluate the pathological changes in tumors. Briefly, the separated tumors from mice were washed with PBS for three times, fixed in 4% paraformaldehyde for 30 min, dehydrated with a graded series of ethanol, infiltrated with xylene, and then embedded in paraffin before being cut into 4-μm thick sections. The prepared sections were stained using H&E following the routine staining procedure and examined using a microscope (Nikon E100; Nikon Corp).

2.10. Immunohistochemical detection of WWP1

The sections were deparaffinized, rehydrated, and then incubated in 3% H_2O_2 to quench endogenous peroxidase activity. After blocked with normal goat serum at room temperature for 30 min, the sections were incubated with a primary antibody against WWP1 (1:300; Proteintech Group, Chicago, IL, USA) overnight at 4 °C, followed by a biotinylated secondary antibody at room temperature for 1 h. Then samples were stained with diaminobenzidine (DAB) for 5 min, counterstained with hematoxylin for 30 s, dehydrated, and then embedded in paraffin. The sections were analyzed using a microscope (Nikon E100; Nikon Corp).

2.11. RNA extraction and qRT-PCR analysis

Total RNA was extracted from glioma cells, human or mouse tissues using TRIzol reagent (Invitrogen, Carlsbad, CA, USA), and was reverse-transcribed to cDNA using the High Capacity cDNA reverse transcription kit (Applied Biosystems, Carlsbad, CA, USA). The cDNA templates were amplified using SYBR Green Real-time PCR Master Mix (TOYOBO, Japan) performing on an ABI 7500 Real-Time PCR system (Applied Biosystems). Relative expression of candidate genes was calculated by the $2^{-\Delta\Delta Ct}$ method. GAPDH was used as internal controls for WWP1. U6 snRNA was used as internal controls for miR-30a-5p.

2.12. Western blot

Total protein from glioma cells, human or mouse tissues was extracted by lysis buffer. After being blocked with 5% skim milk, Aliquots of 20 μg protein were separated with 10% sodium dodecyl sulfate-polyacrylamide gel electrophoresis (SDS-PAGE) and electro-transferred to polyvinylidene fluoride (PVDF) membranes. The membranes were incubated with primary antibodies against p65 (1:500; Santa Cruz Biotechnology Inc., Dallas, TX, USA), p-p65 (1:500; Abcam, Cambridge, MA, USA), overnight at 4 °C, followed by incubation with horseradish peroxidase (HRP)-conjugated secondary antibodies (1:2000; Santa Cruz Biotechnology Inc.) at room temperature for 2 h. Blots were examined by an Enhanced Chemiluminescence (ECL) Detection kit (Pierce Biotechnology, USA) and the band intensity was analyzed by Image-Pro Plus 6.0 software. GAPDH served as the loading control.

2.13. Statistical analysis

The quantitative statistics presented here were calculated as the mean ± standard deviation (SD) from three independent experiments. Statistical analysis was performed using GraphPad Prism version 6 (GraphPad Software; La Jolla, CA). Comparisons between different groups were analyzed using Student's t-test, one-way analysis of variance. $p < 0.05$ was considered to indicate a statistically significant difference.

3. Results

3.1. Expression of WWP1, miR-30a-5p, and p-p65 in glioma tissues

The expression of miR-30a-5p was significantly higher in most glioma tissues than that in normal brain tissues (Fig. 1A). However, compared with the normal brain tissues, the expression of WWP1 in glioma tissues was significantly downregulated, at both mRNA (Fig. 1B) and protein levels (Fig. 1D). We also found that the WWP1 mRNA level was negatively correlated with miR-30a-5p expression in glioma tissues (Fig. 1C). Furthermore, the phosphorylation level of p65 was increased in glioma tissues compared with the normal brain tissues (Fig. 1D). Moreover, compared with the normal human astrocytes (NHA), the expression of WWP1 in glioma cell lines (U87, U251, U138, LN229) was also notably downregulated, at both mRNA (Fig. 1E) and protein levels (Fig. 1F).

3.2. WWP1 overexpression inhibited glioma cell proliferation, migration, and invasion

To determine the functional role of WWP1 in glioma development, we overexpressed WWP1 by transfecting pcDNA3.1-WWP1 into U251 and LN229 cells, which expressed lower WWP1 level. The overexpression efficiency was confirmed by qRT-PCR **(Supplementary** Fig. 1**)**. MTT assay revealed that the growth of U251 cells transfected with pcDNA3.1-WWP1 was significantly impaired compared with those transfected with empty vector (Fig. 2A**)**. Furthermore, Transwell migration and invasion assays indicated that the number of migrated and invaded (Fig. 2C**)** cells in U251 cells transfected with pcDNA3.1-WWP1 was notably less than that in those transfected with empty vector. Similar results were observed in LN229 cells (Fig. 2**B and D)**.

3.3. WWP1 overexpression downregulated miR-30a-5p expression and p65 phosphorylation

We next determined the effect of WWP1 expression on expression of miR-30a-5p and phosphorylation level of p65. Data demonstrated that WWP1 overexpression significantly downregulated miR-30a-5p expression in both U251 (Fig. 3A**)** and LN229 cells (Fig. 3B**)**. Furthermore, WWP1 overexpression led to a significant decrease in p65 phosphorylation level, in both U251 (Fig. 3C**)** and LN229 cells (Fig. 3D).

3.4. miR-30a-5p promoted glioma cell proliferation, migration, and invasion via targeting WWP1

Results of luciferase activity assay showed that the miR-30a-5p mimic significantly decreased luciferase activity in the WWP1-WT group, whereas had no obvious effect on luciferase activity in the WWP1-MIUT group, indicating that WWP1 3′-UTR was directly targeted by miR-30a-5p (Fig. 4A**)**. Moreover, miR-30a-5p mimic significantly increased miR-30a-5p expression (Fig. 4B**),** but decreased the mRNA (Fig. 4C**)** and protein levels of WWP1 (Fig. 4D**)** in LN229 cells. In contrast, miR-30a-5p inhibitor exerted the opposite effect (Fig. 4**B-D)**.

In addition, miR-30a-5p mimic markedly promoted cell proliferation (Fig. 4E**)**, migration (Fig. 4**F and H)**, and invasion (Fig. 4**G and I)** of LN229 cells. In contrast, WWP1 overexpression exerted the opposite effect and abrogated the miR-30a-5p mimic-mediated promotion of cell proliferation (Fig. 4E**)**, migration (Fig. 4**F and H)**, and invasion (Fig. 4**G and I)**. These data indicate that miR-30a-5p may promote glioma cell proliferation, migration, and invasion, at least partially, via inhibiting WWP1.

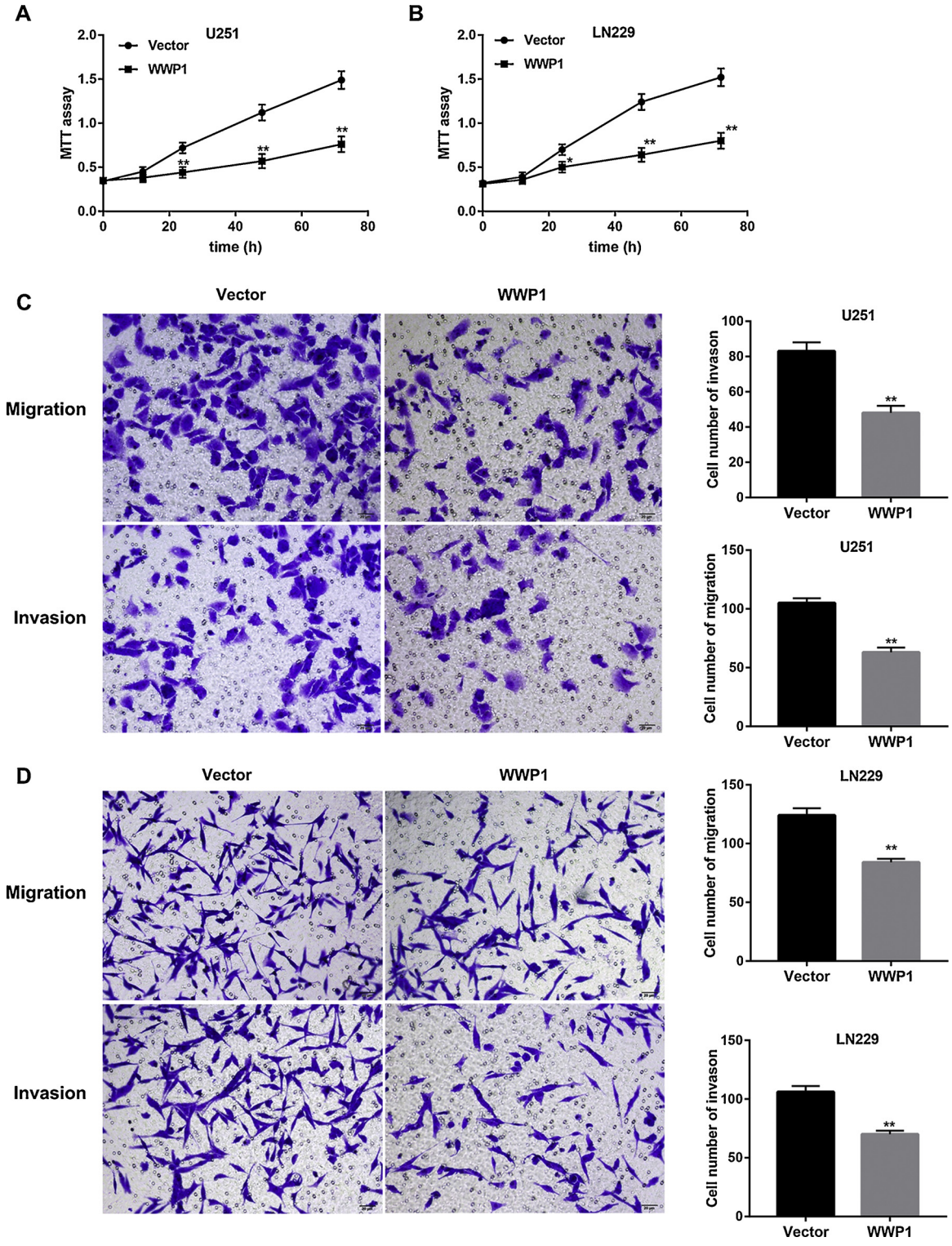

Fig. 2. Effect of WWP1 overexpression on glioma cell proliferation, migration, and invasion.
U251 and LN229 cells were transfected with pcDNA3.1-WWP1 and empty pcDNA3.1 vector. Then cell proliferation (A and B), migration and invasion (C and D) were examined by MTT assay, Transwell migration and invasion assay, respectively. $^{*}P < 0.05$, $^{**}P < 0.01$ vs. Vector group. Results are expressed as mean ± SD for three independent experiments.

3.5. miR-30a-5p was activated by NF-κB through direct binding of NF-κB RelA subunit to the promoter of miR-30a-5p

CHIP assay confirmed the binding of NF-κB p65 to the miR-30a-5p promoter (Fig. 5A). Results of luciferase activity assay revealed that NF-κB RelA overexpression caused a significant increase in luciferase activity in the WT group when compared with the empty vector group. However, NF-κB RelA overexpression exerted no obvious effect on luciferase activity in the MUT group (Fig. 5B). These data verified the binding of NF-κB RelA subunit to the promoter of miR-30a-5p. Furthermore, NF-κB p65 overexpression significantly upregulated miR-30a-5p expression (Fig. 5C), which indicate that miR-30a-5p is

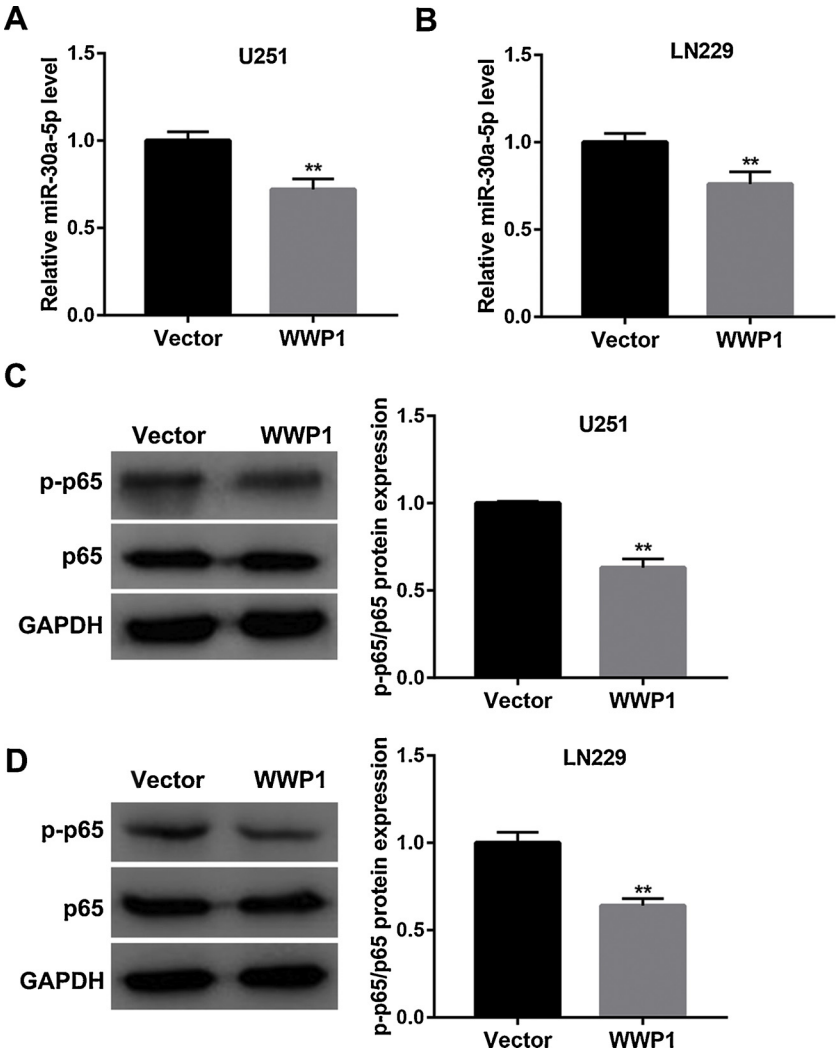

Fig. 3. Effect of WWP1 overexpression on miR-30a-5p expression and p65 phosphorylation.
U251 and LN229 cells were transfected with pcDNA3.1-WWP1 and empty pcDNA3.1 vector. The relative miR-30a-5p expression in U251 (A) and LN229 (B) cells was examined using qRT-PCR. The protein expression of p65, phosphorylated (p)-p65 in U251 (C) and LN229 (D) cells was examined using western blot. $^{**}P < 0.01$ vs. Vector group. Results are expressed as mean ± SD for three independent experiments.

activated by NF-κB through direct binding of NF-κB RelA subunit to the promoter of miR-30a-5p.

3.6. NF-κB p65 overexpression inhibited WWP1 expression and promoted glioma cell proliferation, migration, and invasion via inducing miR-30a-5p transcription

We next sought to investigate the role of NF-κB in regulating malignant behaviors of glioma cells and to clarify whether miR-30a-5p was implicated in this process. Data revealed that miR-30a-5p inhibitor significantly abolished the NF-κB p65 overexpression overexpression-mediated decrease in WWP1 mRNA expression (Fig. 5D). Furthermore, in contrary to p65 overexpression, miR-30a-5p inhibitor notably inhibited cell proliferation (Fig. 5E), migration (Fig. 5**F and H**), and invasion (Fig. 5**G and I**) in LN229 cells. Importantly, miR-30a-5p inhibitor effectively abrogated the p65 overexpression-mediated promotion of glioma cell proliferation, migration, and invasion (Fig. 5**E-I**). Together, these data suggest that NF-κB p65 overexpression inhibited WWP1 expression and promoted glioma cell proliferation, migration, and invasion, at least partially, via inducing miR-30a-5p transcription.

3.7. WWP1 overexpression decreased miR-30a-5p expression and inhibited glioma cell proliferation, migration, and invasion via inhibiting NF-κB p65

Evidence suggests that WWP1 inhibits NF-κB activation by inducing K48-linked polyubiquitination of endogenous TRAF6 (Lin et al., 2013). Here, our results confirmed the inhibition of NF-κB by WWP1 (Fig. 3**C and D**). Additionally, NF-κB can participate in tumor development (Wang et al., 2018). Thus, we here determined whether NF-κB was involved in the WWP1 overexpression-mediated decrease of miR-30a-5p expression and inhibition of glioma cell malignant behaviors. Data revealed that NF-κB p65 overexpression significantly restored the WWP1 overexpression-mediated decrease in miR-30a-5p expression (Fig. 6A).

Furthermore, in contrary to WWP1 overexpression, p65 overexpression significantly facilitated cell proliferation (Fig. 6C), migration (Fig. 6**D and F**), and invasion (Fig. 6**E and G**) in LN229 cells. Of note, p65 overexpression effectively abolished the WWP1 overexpression-mediated inhibition of glioma cell proliferation, migration, and invasion (Fig. 6**C-G**). Collectively, these data indicate that WWP1 overexpression decreases miR-30a-5p expression and inhibits glioma cell proliferation, migration, and invasion, at least in part, via inhibiting NF-κB p65.

In addition to the inhibition of NF-κB by WWP1 (Fig. 3**C and D**), our

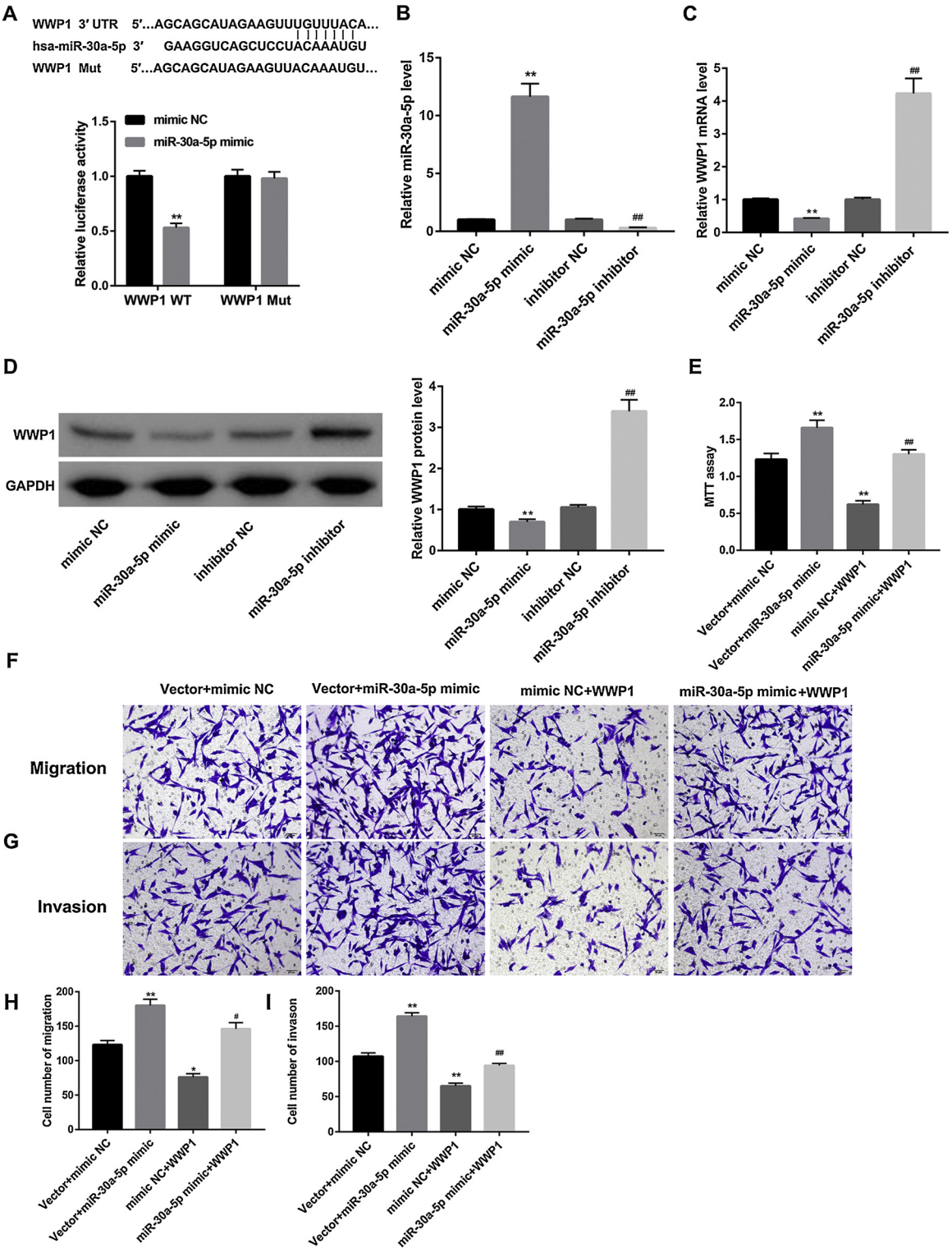

Fig. 4. miR-30a-5p promoted glioma cell proliferation, migration, and invasion via inhibiting WWP1.
(A) Results of luciferase activity assay showed that 3′-UTR of WWP1 was directly targeted by miR-30a-5p. $^{**}P < 0.01$ vs. WWP1 WT + mimic NC group. Effect of miR-30a-5p mimic/inhibitor on miR-30a-5p level (B), the mRNA (C) and protein (D) levels of WWP1 in LN229 cells. $^{**}P < 0.01$ vs. mimic NC group; $^{\#\#}P < 0.01$ vs. inhibitor NC group. Effect of miR-30a-5p mimic or/and WWP1 overexpression on cell proliferation detected by MTT assay (E), cell migration (F) and invasion (G) detected by Transwell assays in LN229 cells. The cell number of migration (H) and invasion (I) was counted from 5 random fields of each well. $^{*}P < 0.05$, $^{**}P < 0.01$ vs. Vector + mimic NC group; $^{\#}P < 0.05$, $^{\#\#}P < 0.01$ vs. Vector + miR-30a-5p mimic group. Results are expressed as mean ± SD for three independent experiments.

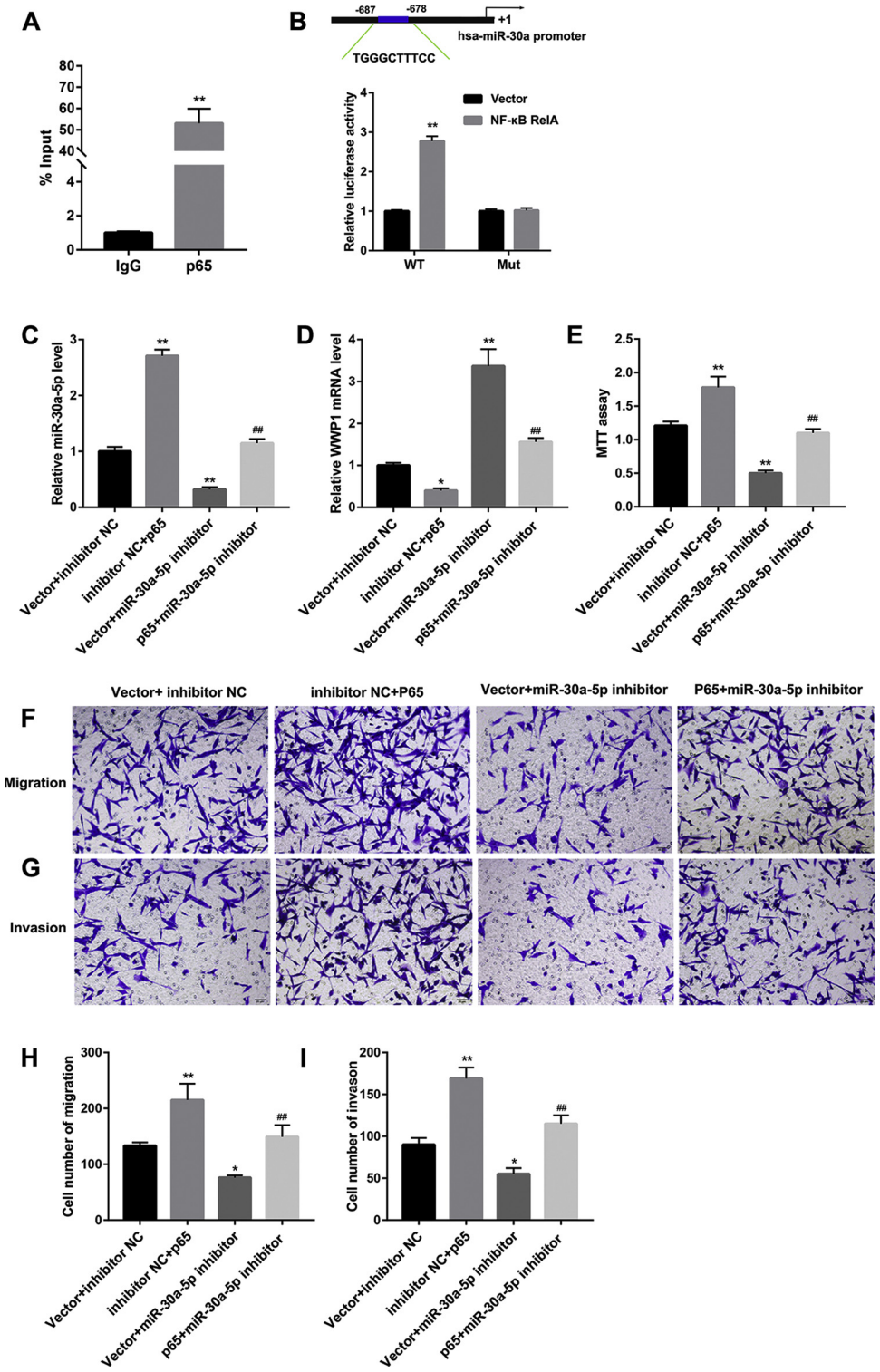

Fig. 5. NF-κB p65 overexpression inhibited WWP1 expression and promoted glioma cell proliferation, migration, and invasion via inducing miR-30a-5p transcription.
(A) CHIP analysis confirmed the binding of NF-κB p65 on miR-30a-5p promoter. $^{**}P < 0.01$ vs. IgG group. (B) Results of luciferase activity assay further verified the binding of NF-κB to the promoter of miR-30a-5p. $^{**}P < 0.01$ vs. WT + Vector group. LN229 cells were transfected with pcDNA3.1-p65 and miR-30a-5p inhibitor, both alone and in combination. Relative miR-30a-5p expression (C) and WWP1 mRNA level (D) were examined by qRT-PCR. (E) Cell proliferation was examined using MTT assay. Cell migration (F) and invasion (G) were examined using Transwell assays. The cell number of migration (H) and invasion (I) was counted from 5 random fields of each well. $^{*}P < 0.05$, $^{**}P < 0.01$ vs. Vector + inhibitor NC group; $^{\#\#}P < 0.01$ vs. inhibitor NC + p65 group. Results are expressed as mean ± SD for three independent experiments.

results also showed that p65 overexpression diminished the WWP1 overexpression-mediated elevation in WWP1 expression (Fig. 6B). This confirmed the reciprocal inhibition between WWP1 and NF-κB, further indicating that miR-30a-5p/WWP1/NF-κB positive feedback loop exists in LN229 cells.

3.8. WWP1 inhibited in vivo growth of xenograft tumors of glioma cells

Finally, we established xenograft mouse models to determine the biological effect of WWP1 overexpression on the tumorigenicity of LN229 cells *in vivo*. The immunohistochemical analysis of WWP1 expression showed that the tumor tissues in the WWP1 OE group exhibited increased expression of WWP1 when compared with the Empty vector group (Fig. 7C). Importantly, the tumors formed in the WWP1 OE group were substantially smaller in volume than those in the Empty vector group (Fig. 7A). Furthermore, the tumors formed in the WWP1 OE group displayed smaller nuclei and the shallower stain as evidenced by H&E staining (Fig. 7B). These data indicate that WWP1 overexpression inhibits the tumorigenicity of LN229 cell *in vivo*.

In addition, the tumors formed in the WWP1 OE group showed

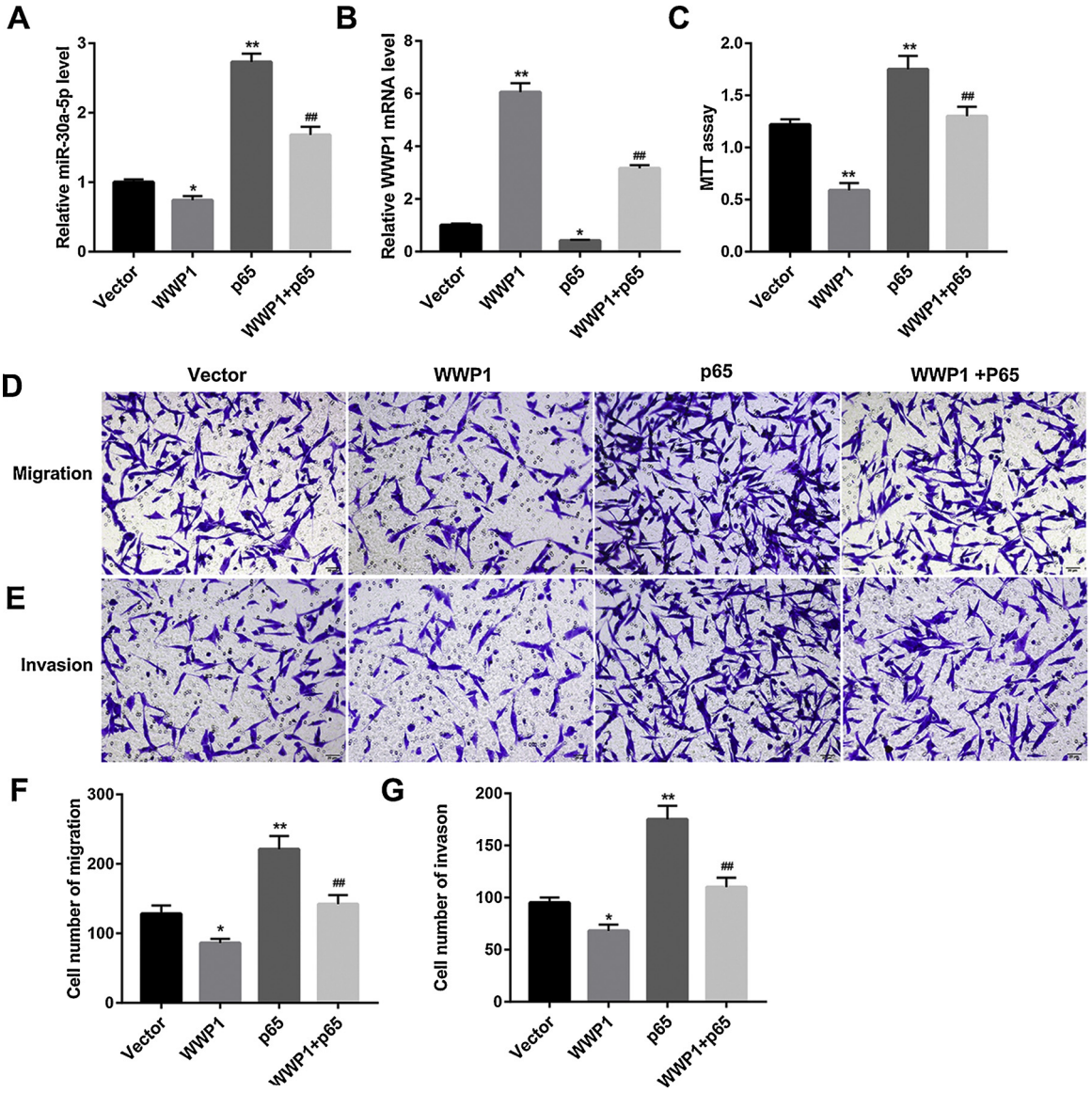

Fig. 6. WWP1 overexpression decreased miR-30a-5p expression and inhibited glioma cell proliferation, migration, and invasion via inhibiting NF-κB p65. LN229 cells were transfected with pcDNA3.1-p65 and pcDNA3.1-WWP1, both alone and in combination. Relative miR-30a-5p expression (A) and WWP1 mRNA level (B) were examined by qRT-PCR. (C) Cell proliferation was examined using MTT assay. Cell migration (D) and invasion (E) were examined using Transwell assays. The cell number of migration (F) and invasion (G) was counted from 5 random fields of each well. $^{*}P < 0.05$, $^{**}P < 0.01$ vs. Vector group; $^{\#\#}P < 0.01$ vs. WWP1 group. Results are expressed as mean ± SD for three independent experiments.

significantly decreased miR-30-5p expression when compared with the Empty vector group (Fig. 7D). Moreover, WWP1 overexpression caused a marked decrease in level of p65 phosphorylation (Fig. 7E). These results further confirmed the involvement of miR-30-5p and NF-κB in WWP1-mediated inhibition of glioma development.

4. Discussion

To our knowledge, this study provided the first evidence that WWP1 was decreased in glioma tissues and glioma cell lines. Furthermore, WWP1 overexpression inhibited glioma cell proliferation, migration, and invasion *in vitro* and slowed glioma cell growth *in vivo*. Our findings are contrary to previous studies which have suggested that WWP1 generally act as an oncogene in multiple cancers (Chen and Zhang, 2018; Goto et al., 2016, Ma, Chen, 2018a). For instance, WWP1 was upregulated in prostate cancer clinical specimens and knockdown of WWP1 inhibited the migration and invasion of prostate cancer cells (Goto et al., 2016). The reasons for this discrepancy in findings are unclear but may relate to differences in cancer type and cell types.

Contrary to the decreased WWP1 expression in glioma tissues and cells, previous studies have demonstrated that miR-30a-5p is over-expressed in glioma cell lines and glioma samples (Wang et al., 2013). Furthermore, contrary to the gliomagenesis-inhibiting activity of WWP1 overexpression, miR-30a-5p promotes glioma cell growth and invasion (Jia et al., 2013; Wang et al., 2015). Importantly, the findings in this study confirmed that miR-30a-5p targeted WWP1 and decreased WWP1 expression at both mRNA and protein level. Furthermore, WWP1 overexpression caused a significant abrogation of miR-30a-5p-mediated promotion of glioma cell proliferation, migration, and invasion. Thus, our results suggest a miR-30a-5p-WWP1 axis in regulating glioma development.

Importantly, one of the most interesting findings from this study is that NF-κB can also regulate miR-30a-5p expression. NF-κB is a homo- or heterodimeric complex formed by the Rel-like domain-containing proteins RelA/p65, RelB, NF-κB1/p105, NF-κB1/p50, Rel, and NF-κB2/p52. NF-κB is a pleiotropic transcription regulator that is activated by

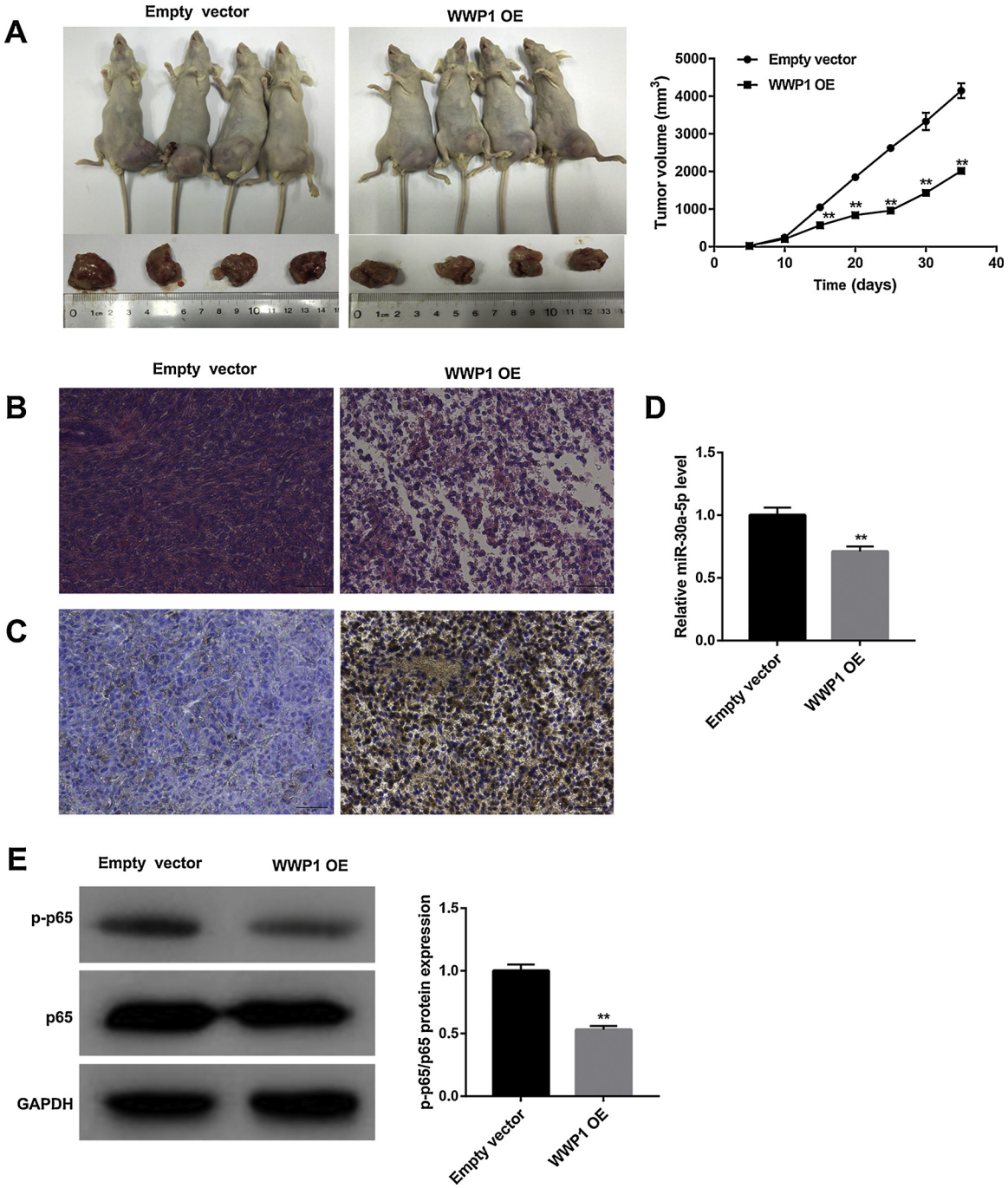

Fig. 7. WWP1 inhibited *in vivo* growth of xenograft tumors of glioma cells.
The LN229 cells transfected with pcDNA3.1-WWP1 (WWP1 OE group) or empty pcDNA3.1 vector (Empty vector group) were injected into mice (n = 4 for each group). Thirty-five days later, the tumors from mice were separated. (A) Subcutaneous tumor appearance of tumor-bearing mice and morphological observation after tumor isolation. Tumor volume was calculated. (B) H&E staining was used to observe the pathological morphology of tumor tissues. (C) Immunohistochemical analysis of WWP1 expression in tumor tissues. (D) The relative miR-30a-5p expression in tumor tissues was examined using qRT-PCR. (E) The protein expression of p65 and phosphorylated (p)-p65 in tumor tissues was examined using western blot. $^{**}P < 0.01$ vs. Empty vector group.

various intra- and extra-cellular stimuli (O'Dea and Hoffmann (2010)). Activated NF-κB translocates into the nucleus and stimulates the expression of genes involved in a wide variety of biological functions (De, 2016). Studies have shown that NF-κB can participate in tumor development by regulating the transcription of certain miRNAs (Li et al., 2017; Shuang et al., 2017; Wang et al., 2018). On the other hand, miR-30a-5p can be activated by certain transcriptional factor. For instance, miR-30a-5p can be activated by Wnt/β-catenin pathway through direct binding of β-catenin/TCF4 to the promoter region of miR-30a-5p (Wang et al., 2015). Intriguingly, our further analysis revealed that miR-30a-5p could be activated by NF-κB through direct binding of NF-κB RelA subunit to the promoter of miR-30a-5p. This links miR-30a-5p and NF-κB, suggesting a direct activation of miR-30a-5p by NF-κB.

Levels of NF-κB activity are much higher in glioma tissues compared with non-glioma tissues, and correspond with increasing grade in astrocytic tumors (Wang et al., 2004). This indicates a strong correlation between constitutive NF-κB activation and gliomagenesis (Atkinson et al., 2010). It has also been demonstrated that inhibition of NF-κB

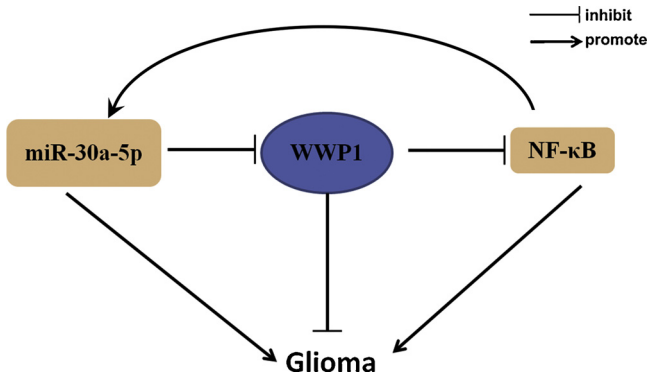

Fig. 8. A possible miR-30a-5p/WWP1/NF-κB positive feedback loop in glioma. WWP1 has been shown to inhibit NF-κB activation, which was confirmed in this study. Our results also showed that WWP1 acts as one of targets of miR-30a-5p. Furthermore, NF-κB activates miR-30a-5p through direct binding of NF-κB RelA subunit to the promoter of miR-30a-5p. Collectively, miR-30a-5p targets WWP1, leading to the upregulation of NF-κB signaling. Activated NF-κB could then, in turn, upregulate miR-30a-5p expression, which forms a miR-30a-5p/WWP1/NF-κB positive feedback loop and regulates glioma development.

activity or of NF-κB-regulated genes reduces the invasive ability of glioma cells (Song et al., 2012). Of note, previous studies have revealed that WWP1 inhibits LPS-induced NF-κB activation by inducing K48-linked polyubiquitination of endogenous TRAF6 (Lin et al., 2013). Our results confirmed that NF-κB p65 phosphorylation was inhibited by WWP1. Besides, we also found that NF-κB p65 overexpression effectively abolished the WWP1 overexpression-mediated inhibition of glioma cell proliferation, migration, and invasion. Therefore, these findings support the notion that WWP1 suppresses glioma development, at least in part, by inhibiting NF-κB. However, whether the mechanism by which WWP1 inhibits NF-κB activation in glioma needs further investigation.

Furthermore, our results showed that miR-30a-5p mimic decreased WWP1 expression, whereas WWP1 overexpression downregulated miR-30a-5p via inhibiting p65 phosphorylation, indicating that a reciprocal negative regulation exists between WWP1 and miR-30a-5p. Furthermore, we also found the reciprocal inhibition between WWP1 and NF-κB. These data suggest that miR-30a-5p/WWP1/NF-κB positive feedback loop exists in LN229 cells (Fig. 8). Moreover, our *in vivo* experiments verified that WWP1 overexpression inhibited *in vivo* growth of xenograft tumors of glioma cells LN229, accompanied with a decrease in miR-30-5p and NF-κB p65 phosphorylation. This further indicates the possible WWP1-NF-κB-miR-30a-5p axis in regulating glioma development *in vivo*.

In conclusion, our findings demonstrate miR-30a-5p targets WWP1, leading to the upregulation of NF-κB signaling, thereby promoting glioma development. Activated NF-κB could then, in turn, upregulate miR-30a-5p expression, which forms a positive feedback loop. Thus, the "miR-30a-5p-WWP1-NF-κB" positive feedback loop plays an important role in regulating the malignant behavior of glioma cells, and might provide a potential therapeutic strategy for treating glioma.

Conflict of interest

All the authors declare no conflict of interest.

Acknowledgments

None.

Appendix A. Supplementary data

Supplementary material related to this article can be found, in the online version, at doi:https://doi.org/10.1016/j.biocel.2019.04.003.

References

Allen, I.C., Wilson, J.E., Schneider, M., Lich, J.D., Roberts, R.A., Arthur, J.C., et al., 2012. NLRP12 suppresses colon inflammation and tumorigenesis through the negative regulation of noncanonical NF-kappaB signaling. Immunity 36, 742–754.
Atkinson, G.P., Nozell, S.E., Benveniste, E.T., 2010. NF-kappaB and STAT3 signaling in glioma: targets for future therapies. Expert Rev. Neurother. 10, 575–586.
Chen, C., Sun, X., Guo, P., Dong, X.Y., Sethi, P., Zhou, W., et al., 2007. Ubiquitin E3 ligase WWP1 as an oncogenic factor in human prostate cancer. Oncogene 26, 2386–2394.
Chen, J., Zhang, W., 2018. High expression of WWP1 predicts poor prognosis and associates with tumor progression in human colorectal cancer. Am. J. Cancer Res. 8, 256–265.
De, L.F., 2016. Role of nuclear factor kappa B (NF-κB) in growth plate chondrogenesis. Pediatr. Endocrinol. Rev. 13, 720–730.
DeWitt, J.C., Jordan, J.T., Frosch, M.P., Samore, W.R., Iafrate, A.J., Louis, D.N., et al., 2017. Cost-effectiveness of IDH testing in diffuse gliomas according to the 2016 WHO classification of tumors of the central nervous system recommendations. Neuro-oncology 19, 1640–1650.
Deyao, W.U., Zhou, Y., Pan, H., Zhou, J., Fan, Y., Ping, Q.U., 2014. microRNA-99a inhibiting cell proliferation, migration and invasion by targeting fibroblast growth factor receptor 3 in bladder cancer. Oncol. Lett. 7, 1219–1224.
Goto, Y., Kojima, S., Kurozumi, A., Kato, M., Okato, A., Matsushita, R., et al., 2016. Regulation of E3 ubiquitin ligase-1 (WWP1) by microRNA-452 inhibits cancer cell migration and invasion in prostate cancer. Br. J. Cancer 114, 1135–1144.
Huang, J., Chen, H., Wei, Q., Zhang, Z., Zhong, Z., Xu, Y., 2017. Downregulation of LKB1 promotes tumor progression and predicts unfavorable prognosis in patients with glioma. Oncol. Lett. 13, 1688–1694.
Jia, Z., Wang, K., Wang, G., Zhang, A., Pu, P., 2013. MiR-30a-5p antisense oligonucleotide suppresses glioma cell growth by targeting SEPT7. PLoS One 8, e55008.
Ku, T., Li, B., Gao, R., Zhang, Y., Yan, W., Ji, X., et al., 2017. NF-κB-regulated microRNA-574-5p underlies synaptic and cognitive impairment in response to atmospheric PM (2.5) aspiration. Part. Fibre Toxicol. 14, 34.
Li, L., Kim, I., Chiasson, V., Chatterjee, P., Gupta, S., 2017. NF-κB mediated miR-130a modulation in lung microvascular cell remodeling: Implication in pulmonary hypertension. Exp. Cell Res. 359, 235–242.
Lin, X.W., Xu, W.C., Luo, J.G., Guo, X.J., Sun, T., Zhao, X.L., et al., 2013. WW domain containing E3 ubiquitin protein ligase 1 (WWP1) negatively regulates TLR4-mediated TNF-Î ± and IL-6 production by proteasomal degradation of TNF receptor associated factor 6 (TRAF6). PLoS One 8, e67633.
Ma, L., Chen, X., Li, C., Cheng, R., Gao, Z., Meng, X., et al., 2018a. miR-129-5p and -3p co-target WWP1 to suppress gastric cancer proliferation and migration. J. Cell. Biochem.
Ma, M., Pei, Y., Wang, X., Feng, J., Zhang, Y., Gao, M.Q., 2018b. LncRNA XIST mediates bovine mammary epithelial cell inflammatory response via NF-kappaB/NLRP3 inflammasome pathway. Cell Prolif., e12525.
O'Dea, E., Hoffmann, A., 2010. NF-κB Signaling. Wiley Interdisciplinary Reviews Systems Biology & Medicine 1. pp. 107–115.
Shuang, T., Wang, M., Zhou, Y., Shi, C., Wang, D., 2017. NF-κB1, c-Rel, and ELK1 inhibit miR-134 expression leading to TAB1 upregulation in paclitaxel-resistant human ovarian cancer. Oncotarget 8, 24853–24868.
Song, L., Liu, L., Wu, Z., Lin, C., Dai, T., Yu, C., et al., 2012. Knockdown of stomatin-like protein 2 (STOML2) reduces the invasive ability of glioma cells through inhibition of the NF-kappaB/MMP-9 pathway. J. Pathol. 226, 534–543.
van Delft, M.A., Huitema, L.F., Tas, S.W., 2015. The contribution of NF-κB signalling to immune regulation and tolerance. Eur. J. Clin. Invest. 45, 529–539.
Wang, H., Wang, H., Zhang, W., Huang, H., S L Liao, W., N Fuller, G., 2004. Analysis of the Activation Status of Akt, NFB, and Stat3 in Human Diffuse Gliomas.
Wang, K., Jia, Z., Zou, J., Zhang, A., Wang, G., Hao, J., et al., 2013. Analysis of hsa-miR-30a-5p expression in human gliomas. Pathol. Oncol. Res. 19, 405–411.
Wang, Z., Dai, X., Chen, Y., Sun, C., Zhu, Q., Zhao, H., et al., 2015. MiR-30a-5p is induced by Wnt/β-catenin pathway and promotes glioma cell invasion by repressing NCAM. Biochem. Biophys. Res. Commun. 465, 374–380.
Wang, S., Li, Z., Chen, Q., Wang, L., Zheng, J., Lin, Z., et al., 2018. NF-κB-induced MicroRNA-211 inhibits interleukin-10 in macrophages of rats with lipopolysaccharide-induced acute respiratory distress syndrome. Cell. Physiol. Biochem. 45, 332–342.